Acta Mechanica Solida Sinica (2022) 35:746–754
https://doi.org/10.1007/s10338-022-00319-2

Effective Energy Density of Glass Rejuvenation

Gan Ding[1,2] · Feng Jiang[1] · Lanhong Dai[2,3] · Minqiang Jiang[2,3]

Received: 9 January 2022 / Revised: 24 February 2022 / Accepted: 28 February 2022 / Published online: 14 April 2022

Abstract
Glasses with rejuvenated structures usually exhibit improved room-temperature plasticity, which facilitates their applications. However, glass rejuvenation requires external energy injection to "shake up" the frozen-in disordered structure. In this work, we give the answer to how much the required energy is. According to the constitutive model of amorphous plasticity, we find that the applied stress higher than the steady-state flow value can effectively induce the structural disordering in terms of the generation of free volume. Therefore, the effective energy density (EED) of structural rejuvenation is defined as the integral of this effective stress on the corresponding strain. By tailoring the applied strain, strain rate, temperature and initial free volume, different degrees of structural rejuvenation are achieved, which show a generally linear correlation with the defined EED. This work deepens the understanding of glass rejuvenation from an energy perspective.

Keywords Glass · Structural rejuvenation · Effective energy density · Shear transformations · Free volume

1 Introduction

From a potential energy landscape perspective, glasses or disordered solids reside in "fragile" basins that are thermodynamically metastable [1–3]. Therefore, glasses will spontaneously age into the deeper "strong" basins. This physical aging process usually induces mechanical brittleness, severely deteriorating the wide applications of glasses as structural materials. Intriguingly, aged glasses can be structurally rejuvenated by thermo-mechanical activation, which results in the recovery of both relaxation enthalpy and global plasticity [4–7]. It is thus of both scientific and practical significance to understand the structural rejuvenation of glasses [8–11].

With substantial efforts [12–15], the physical mechanism of glass rejuvenation has been clarified as the creation of atomic free volume via a series of shear transformations (STs), i.e., localized irreversible rearrangements of small groups of atoms. This trans-scale dynamic process requires the injection of external energy to "shake up" the frozen-in disordered configurations, and meanwhile, to avoid aging-induced ordering. At lower stress levels, the external energy is only stored in the elastic matrix of glasses, which cannot contribute to structural disordering permanently. But when the stress reaches a threshold, multitudinous STs will be activated to destroy the confining elastic matrix [16, 17]. In this process, the plastic work can be approximately decomposed into the portion stored in the configurational space and the ordinary heat dissipated via vibrational phonons [18]. The configurational portion of plastic work is, in concept, similar to the "cold work" that directly contributes to the structural softening of shear banding [19]. It is the plastic storage work that effectively contributes to the structural disordering or the generation of excess free volume [13, 20, 21]. So here comes an interesting question: how much energy does it require to achieve structural rejuvenation of glasses?

In this paper, we present a theoretical answer to this question within the framework of the constitutive model of amorphous solids by Jiang et al. [22] By considering the interaction of STs and free volume dynamics, this model reveals a stress threshold of structural disordering that can be determined by the dynamic balance between annihilation and generation of free volume mediated by STs. Therefore, the effective energy density (EED) of structural rejuvenation can be further defined by the integral of the effective stress

✉ Minqiang Jiang
mqjiang@imech.ac.cn

1 State Key Laboratory for Mechanical Behavior of Materials, Xi'an Jiaotong University, Xi'an 710049, China

2 State Key Laboratory of Nonlinear Mechanics, Institute of Mechanics, Chinese Academy of Sciences, Beijing 100190, China

3 School of Engineering Science, University of Chinese Academy of Sciences, Beijing 100049, China

beyond this threshold on the corresponding strain. We apply the defined EED to both constant strain-rate loading and constant stress (creep), and find that the structural rejuvenation degree is approximately linear to the EED in despite of varying conditions such as strain, strain rate, temperature and initial free volume.

2 Definition of Effective Energy Density

Applying mechanical deformation is the most frequently-used method to achieve structural rejuvenation of glasses, especially metallic glasses [6, 23, 24]. In general, the mechanical rejuvenation methods include the constant strain-rate loading and the creep with a constant stress. The two types of deformation can be well described by the constitutive model of amorphous solids [22]. This model considers the interaction between STs and free volume dynamics, and thus can inherently capture the rejuvenation of glassy structure [14].

In order to highlight the essential physics, we consider the quasi-static simple-shear case. The total shear strain is decomposed into elastic and plastic portions, $\dot{\varepsilon} = \dot{\varepsilon}^{el} + \dot{\varepsilon}^{pl}$. The elastic strain obeys Hooke's law, $\varepsilon^{el} = \sigma/\mu$, where σ is the shear stress and μ is the shear modulus. The plastic deformation results from the activation of a series of STs, and the activation rate depends on the combined effect of applied stress, thermal fluctuation and local free volume [25–27]. The plastic strain rate is determined by the dynamic balance of two-state STs along shear "positive" and "negative" directions, which can be expressed as

$$\dot{\varepsilon}^{pl} = \exp\left(-\frac{1}{\xi}\right)\exp\left[E_A\left(1-\frac{1}{T}\right)\right] \times\left[\Lambda\sinh\left(\frac{\sigma}{T}\right)-\Delta\cosh\left(\frac{\sigma}{T}\right)\right] \tag{1}$$

where ξ is the average concentration of free volume, T is temperature, and E_A is the thermal activation energy. The internal state variables Δ and Λ represent the bias and summation of normalized populations of two-state STs, respectively. The dynamic evolution of STs involves the internal reconstruction between two states and the agitation by the plastic deformation, which is expressed as

$$\dot{\Delta} = 2\dot{\varepsilon}^{pl} - \varphi\left|\sigma\dot{\varepsilon}^{pl}\right|\Delta \tag{2}$$

$$\dot{\Lambda} = \varphi\left|\sigma\dot{\varepsilon}^{pl}\right|(1-\Lambda) \tag{3}$$

where φ is a dimensionless coefficient. Furthermore, the free volume dynamics includes the STs-mediated creation and relaxation-induced annihilation [28, 29]. A fraction of the plastic work is transformed into the bulk energy, leading to the creation of free volume. But the annihilation mainly relies on thermal transformations of collective atoms. Therefore, the net creation of the free volume can be calculated as

$$\dot{\xi} = D_{ia}\left|\sigma\dot{\varepsilon}^{pl}\right| - \phi\exp\left(-\frac{1}{\xi}\right)\exp\left[E_a\left(1-\frac{1}{T}\right)\right] \tag{4}$$

where D_{ia} is a dilatancy factor measuring the ability to create the free volume, ϕ is a coefficient that characterizes the efficiency of depleting a free volume, and E_a is the energy barrier of thermal annihilation. Usually, the energy barrier E_A is larger than E_a [30, 31]. Due to the quasi-static loading, the isothermal condition is adopted here and temperature rise is expected to be negligible. The physical mechanism and predictive power of this constitutive model have been extensively studied [14, 26, 32, 33].

We take a typical $Zr_{55}Cu_{30}Ni_5Al_{10}$ metallic glass as a model material for numerical calculations. The mechanical and physical parameters are chosen as [22]: $\mu = 33$ GPa, $T_g = 679$ K, $\phi = 10, \varphi = 0.5, E_A = 3.83$ eV and $E_a = 2.65$ eV. If there is no specific state, the initial system is chosen as: $\Lambda_0 = 0.6$, $\Delta_0 = 0.01$, $D_{ia} = 0.009$, and $\xi_0 = 0.05$. With these parameters, Eqs. (1)–(4) can be numerically integrated at a fixed temperature.

We first calculate the mechanical response during the constant strain-rate loading, where the shear stress is determined by $\dot{\sigma} = \mu(\dot{\varepsilon} - \dot{\varepsilon}^{el})$. Here we normalize the stress by $\sigma_0 = 2k_BT_g/V_a$ and strain by $\varepsilon_0 = n_\infty V_a$, where k_B is the Boltzmann constant, V_a is the ST activation volume, and n_∞ is the total populations of STs in a steady flow state. If there is no specific state, the strain-rate $\dot{\varepsilon}$ is 1.0×10^{-4} s^{-1} and temperature is 0.9 T_g. Figure 1a shows the calculated shear stress–strain curve, which displays a typical stress overshoot behavior. Specifically, as the applied strain increases, the stress increases to a maximum and then decreases towards its steady-state flow value σ_f. The corresponding free volume evolution is calculated in Fig. 1b. With increasing strain, the initial free volume first slightly decreases, then increases after a critical strain ε_c, and finally reaches a saturated value. Obviously, the critical ε_c corresponds to a threshold stress σ_c. It is interesting to find that σ_c is very close to the steady-state flow stress σ_f. Glass rejuvenation is a dynamic process jumping from a lower-energy state to a higher-energy state, so the increase of the potential energy should be the direct judgment of rejuvenation [7, 34]. Besides, there are many indicators of structural rejuvenation, such as free volume [10], effective temperature [35], Voronoi polyhedral [7] and the height of boson peak [14]. Here the degree of structural rejuvenation is simply measured by the amount of STs-mediated free volume. Therefore, when the applied strain exceeds ε_c or $\sigma > \sigma_c$, the glass is structurally rejuvenated. Otherwise, the free volume decreases, indicating a physical aging. Considering this situation, we can define the EED of structural

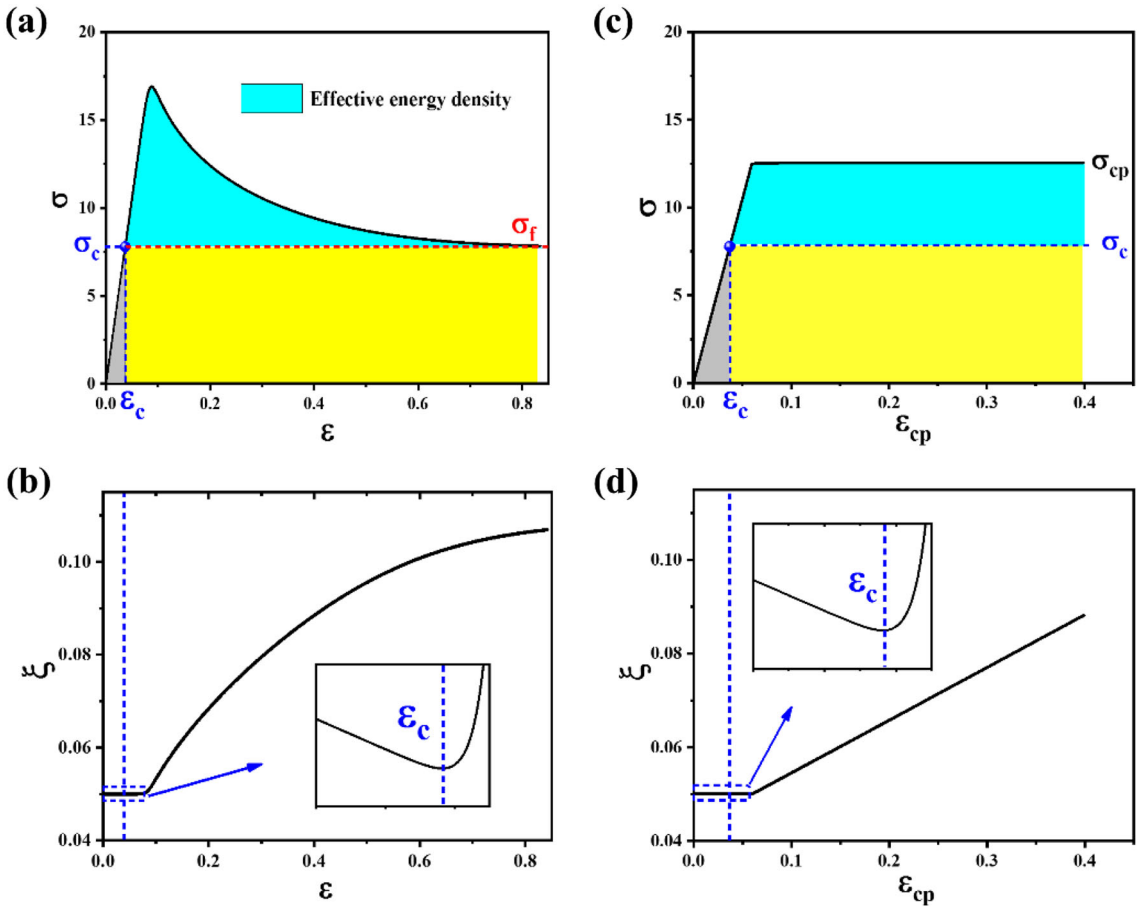

Fig. 1 The definition of effective energy density, where the cyan area denotes the EED: **a** the constitutive behaviors for constant strain-rate test, where the red and blue dashed line represent σ_c and ε_c, respectively; **b** the corresponding evolution of free volume; **c** the constitutive behaviors for creep test; **d** the corresponding evolution of free volume

rejuvenation as an integral of the so-called effective stress $(\sigma - \sigma_c)$ on the corresponding effective strain $(\varepsilon - \varepsilon_c)$, which reads

$$\mathrm{EED} = \int_{\varepsilon_c}^{\varepsilon} (\sigma - \sigma_c)\, \mathrm{d}\varepsilon \tag{5}$$

The cyan area in Fig. 1a is the defined EED. Below σ_c, the reversible elastic energy density (the gray area) is stored in the elastic matrix. Coincidentally, the EED equals to the area of the stress overshoot, so stress overshoot should be an important signal of structural disordering or rejuvenation [36, 37]. It is noted that the yellow area is the "hot work," which is dissipated in the form of heat during the deformation. At the steady-state flow stage, both the EED and free volume reach their respective saturation. Thus further plastic deformation is ineffective for structural rejuvenation, which is consistent with the experimental observations [28, 38, 39].

Next, we define the EED during the creep loading. The loading process includes a fast constant strain-rate load and a subsequent constant stress σ_{cp}, as shown in Fig. 1c. Correspondingly, the time-dependent creep strain ε_{cp} can be measured. In the creep, there is also a stress threshold, only beyond which the structural rejuvenation occurs [13, 21]. Similar to the constant strain-rate test, the stress threshold σ_c and the critical strain ε_c can also be determined according to the balance point of free volume as shown in Fig. 1d. Beyond σ_c, the free volume creation overcomes its annihilation, leading to the structural rejuvenation. Similar to Eq. (5), the EED can be defined for the creep loading, which is also expressed as an integral:

$$\mathrm{EED} = \int_{\varepsilon_c}^{\varepsilon_{cp}} (\sigma_{cp} - \sigma_c)\, \mathrm{d}\varepsilon_{cp} \tag{6}$$

As shown in Fig. 1c, the blue horizontal dashed line denotes σ_c, and the cyan area above σ_c is the EED. Under sup-σ_c creep, only a fraction of the plastic work contributes to configurational changes and structural disordering. During the mechanical rejuvenation in both constant strain-rate loading and creep, the EED results in the accumulation of

excess free volume, but elastic energy (gray area) or dissipated plastic energy (yellow area) does not. Therefore, the EED (the cyan area in Fig. 1) should be the required energy to achieve structural rejuvenation of glasses.

3 Results and Discussion

To rationalize the EED defined above, we explore the relation between the EED and the structural rejuvenation degree under different conditions. According to Eqs. (5) and (6), the EED mainly depends on effective stress and the corresponding strain. In the constant strain-rate test, the constitutive responses are controlled by several parameters, including applied strain, strain rate, temperature and initial free volume. In the creep test, the effective energy density is solely controlled by the creep strain when the creep stress is fixed.

Figure 2a shows the stress–strain curves when deformed to different strains under a constant strain rate of 1.0×10^{-4} s^{-1}. The black horizontal dashed line is σ_c. Meanwhile, the rejuvenation degree can be reflected in the corresponding free volume as shown in the colored circles in Fig. 2b. According to Eq. (5), the EED keeps growing with the increase of applied strain until the stress approaches to the final steady-state flow value. Correspondingly, the free volume also increases gradually with increasing strain, finally reaching its saturation at σ_f.

Figure 2c shows the creep strain response with loading time under sup-σ_c creep (the applied creep stress is in accordance with the creep in Fig. 1c). As expected, the creep strain displays the three-stage behavior: a sudden jump is followed by a gradual increase and the final strain-divergence stage. This theoretical result well reproduces the experimental and atomically simulated observations [30, 40, 41]. Different degrees of structural rejuvenation are achieved by controlling different creep strains. Tailoring the loading time, the applied creep strains (colored circles) are 0.1, 0.15, 0.2, 0.25, 0.3, 0.35 and 0.4, respectively. Figure 2d shows the corresponding free volume with different applied strains during the creep. Obviously, the free volume increases monotonously

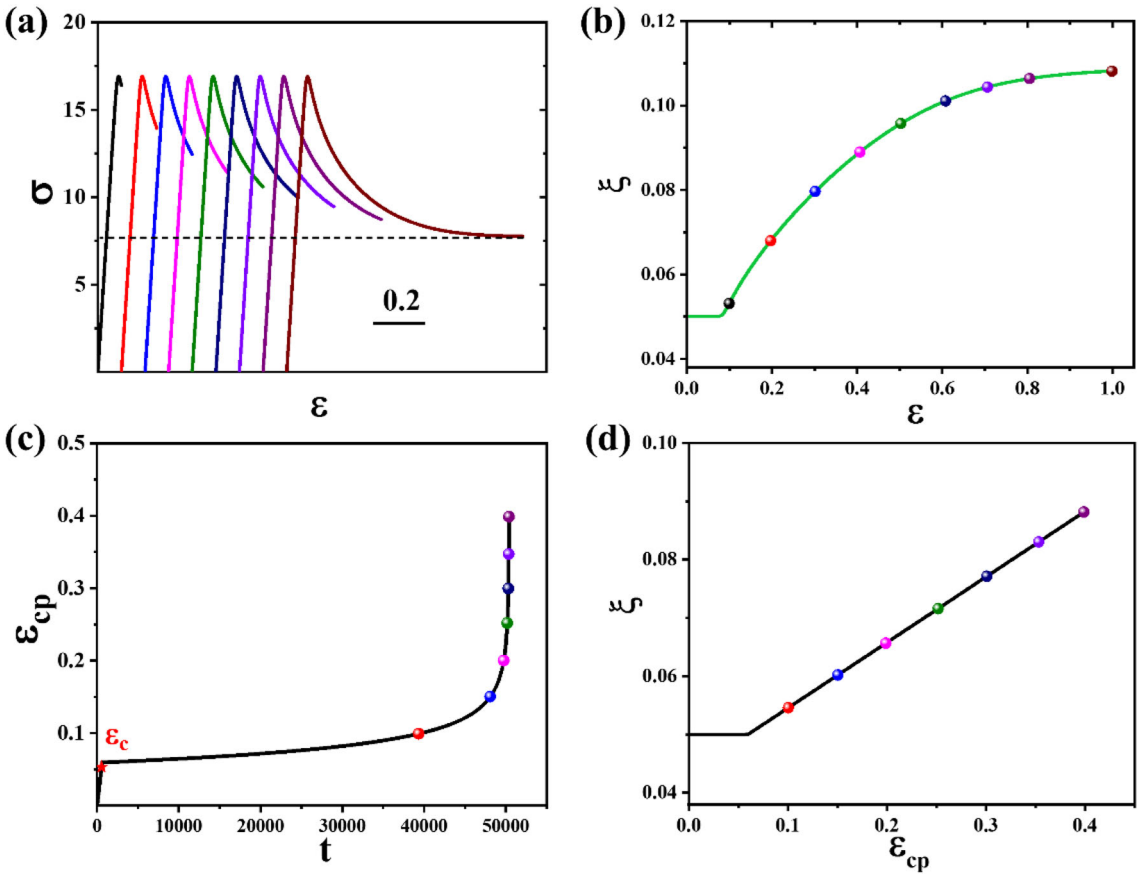

Fig. 2 The effect of applied strain on structural rejuvenation: **a** stress–strain curves of specimens deformed to different strains, where the dashed line donates the stress threshold; **b** the corresponding free volume of specimens deformed to different strains; **c** creep strain response with loading time, where the red star is the critical strain; **d** the corresponding free volumes of specimens with different creep strains

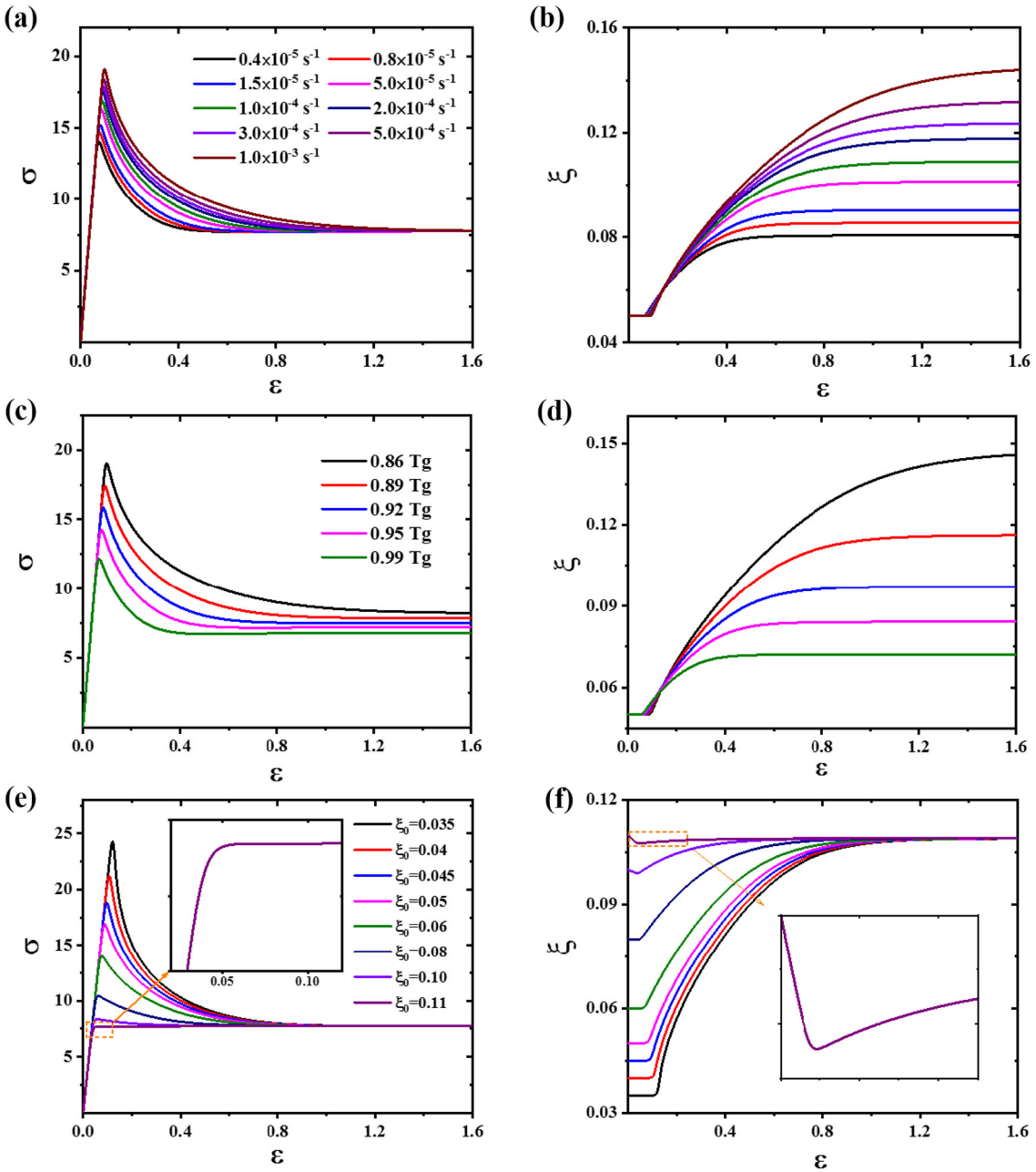

Fig. 3 **a, c, e** The effects of strain-rate, temperature and initial free volume on the constitutive behavior; **b, d, f** the corresponding evolutions of free volume

with the increasing strain. But in real creeps, the glass will undergo mechanical failure corresponding to strain divergence. Therefore, neither creep strain nor rejuvenation degree can increase without any boundaries.

Figure 3a shows the strain-rate dependence of constitutive behaviors at $T = 0.9\,T_g$, where the strain-rate is applied from 0.4×10^{-5} s^{-1} to 1×10^{-3} s^{-1}. It is found that the steady-state flow stress is independent of the applied strain rate. But the peak stress and overshoot become more pronounced at higher strain rate, which results in a higher EED (the area of stress overshoot). Meanwhile, the corresponding rejuvenation degree, that is, the saturation value of free volume, is shown in Fig. 3b. Clearly, the higher strain rate leads to the higher rejuvenation degree. Figure 3c shows the stress–strain curves at varying temperatures, where the strain rate is 1.0×10^{-4} s^{-1}. Obviously, both the peak stress and flow stress show the softening property, and the EED becomes smaller with increasing temperature. The lower saturated free volume in Fig. 3d indicates a lower degree of structural rejuvenation.

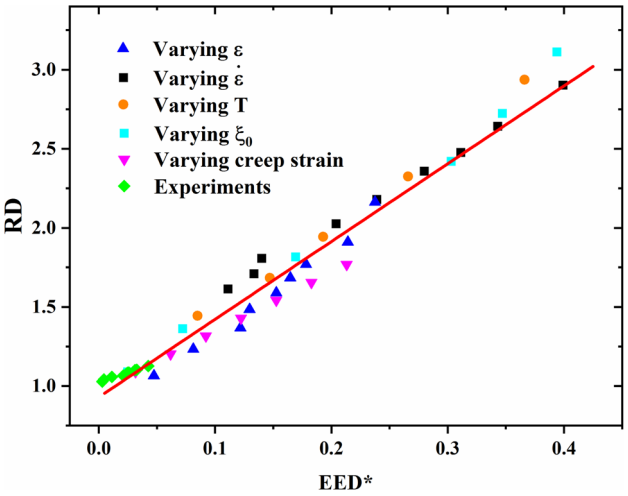

Fig. 4 Correlation between rejuvenation degree and EED* for constant strain-rate and creep tests, where the red straight solid line is a linear fit to the data

Figure 3e displays the stress–strain curves with different initial free volumes ranging from 0.035 to 0.11, where the strain-rate is 1.0×10^{-4} s^{-1} and the temperature is 0.9 T_g. It shows that the threshold stress of rejuvenation or the flow stress has nothing to do with the initial free volume ξ_0. However, the glasses with lower ξ_0 have the larger stress overshoot and EED during the homogeneous deformation. Figure 3f shows that the free volume will reach the identical saturation in the steady-state flow stage regardless of its initial value. This results agree with the findings of Barbot et al. based on atomistic simulations [42]. It reveals that the glasses with lower initial free volume prefer to achieve more pronounced rejuvenation due to a larger EED. On the contrary, the glasses with relatively high free volume ($\xi_0 = 0.11$) present the strain-hardening behavior as shown in the inset of Fig. 3e. This situation has been observed experimentally in a highly-rejuvenated metallic glass [43]. In this situation, there is no effective energy density, and thus structural aging occurs as shown in the inset of Fig. 3f.

In all cases calculated above, the rejuvenation degree shows a positive correlation with the EED in both the quasi-static strain-rate loading and the creep. Such positive correlation is also supported by plastic deformation of amorphous $Pd_{40}Ni_{40}P_{20}$, where the measured overshoots and disordering become more pronounced with increasing strain-rate [44]. In order to demonstrate the universality of the rejuvenation-EED correlation, the rejuvenation degree (RD) here is defined as the normalization of free volume by its initial value, that is, ξ / ξ_0. Also, the EED is normalized by the threshold stress σ_c of rejuvenation, labeled as EED*.

We plot the RD against EED* for all theoretically calculated data and experimental tests, as shown in Fig. 4. The calculated data are shown in Table 1. The experimental results are taken from the literature [44]. Clearly, the RD and EED* show an approximately linear correlation, which can be satisfactorily fitted with the Pearson correlation coefficient of ~0.986. All data collapse onto a general straight line, regardless of applied strain, strain rate, temperature or initial free volume. It is therefore identified that the EED defined in Eq. (5) or (6) is the required energy for structural rejuvenation in glasses.

Obviously, the rejuvenation degree increases monotonously with the effective energy density. Therefore, the glass can be highly rejuvenated as long as the EED* is sufficiently high. For the uniaxial compression or tension, enhanced EED* could be accessible for faster loading or higher strain rate, which speeds up the dynamic process of structural disorder and suppresses the aging [8, 35]. However, the deformation tends to be localized into shear bands with ~ 10-nm thickness at higher strain rate, leading to the inevitable brittle fracture [45–48]. To overcome this issue, we have previously shown that the shock compression with 1D strain state can realize the ultrafast extreme rejuvenation [14]. In addition, triaxial stress states are frequently introduced in the experiments, such as constrained loading [11], high-pressure annealing [49] and cold rolling [6]. The above-mentioned methods not only increase the effective stress but also guarantee large effective strain, thus injecting more stored energy of "cold work" for glass rejuvenation. Under some extreme conditions, when the EED* is increased to a critical value, the bulk of glass is liquid-like due to the excess free volume, which may maximize the degree of rejuvenation.

4 Concluding Remarks

In summary, the mechanical response and rejuvenation behavior are studied on constant strain-rate and creep tests within the theoretical framework of STs and free volume. It reveals that the stress threshold of structural rejuvenation is numerically close to the steady-state flow stress, beyond which the free volume can be significantly generated via STs. Accordingly, we define the EED and investigate its correlation with structural rejuvenation by controlling applied strain, strain rate, temperature and initial free volume. The main conclusions are listed as follows:

(1) The EED of glass rejuvenation is defined as the integral of the effective stress on the corresponding strain. In the constant strain-rate loading, the defined EED is close to the area of the stress overshoot.
(2) The defined EED shows an approximately linear correlation with the rejuvenation degree in terms of the created free volume. Thus the EED is identified as the required energy for glass rejuvenation that can be

Table 1 The σ_c, effective energy density (EED), free volume (ξ_0 and ξ), normalized EED (EED*) and rejuvenation degree (RD) under different deformation conditions

Condition	σ_c	EED	ξ_0	ξ	EED*	RD
0.9 T_g, 10^{-4} s^{-1}	7.78	0.372	0.05	0.0533	0.0474	1.065
0.9 T_g, 10^{-4} s^{-1}	7.78	0.634	0.05	0.0616	0.0813	1.233
0.9 T_g, 10^{-4} s^{-1}	7.78	0.953	0.05	0.0684	0.1218	1.368
0.9 T_g, 10^{-4} s^{-1}	7.78	1.011	0.05	0.0743	0.1296	1.485
0.9 T_g, 10^{-4} s^{-1}	7.78	1.191	0.05	0.0795	0.1527	1.59
0.9 T_g, 10^{-4} s^{-1}	7.78	1.284	0.05	0.0842	0.1646	1.684
0.9 T_g, 10^{-4} s^{-1}	7.78	1.391	0.05	0.0885	0.1782	1.769
0.9 T_g, 10^{-4} s^{-1}	7.78	1.670	0.05	0.0956	0.2141	1.911
0.9 T_g, 10^{-4} s^{-1}	7.78	1.853	0.05	0.1082	0.2376	2.163
0.9 T_g, creep	7.78	0.246	0.05	0.0545	0.0315	1.090
0.9 T_g, creep	7.78	0.482	0.05	0.0602	0.0618	1.203
0.9 T_g, creep	7.78	0.718	0.05	0.0658	0.0921	1.316
0.9 T_g, creep	7.78	0.954	0.05	0.0714	0.1223	1.428
0.9 T_g, creep	7.78	1.192	0.05	0.0771	0.1526	1.541
0.9 T_g, creep	7.78	1.426	0.05	0.0827	0.1828	1.654
0.9 T_g, creep	7.78	1.662	0.05	0.0884	0.2131	1.768
0.9 T_g, 0.4×10^{-5} s^{-1}	7.78	0.861	0.05	0.0807	0.1111	1.614
0.9 T_g, 0.8×10^{-5} s^{-1}	7.78	1.033	0.05	0.0855	0.1335	1.709
0.9 T_g, 1.5×10^{-5} s^{-1}	7.78	1.085	0.05	0.0903	0.1402	1.806
0.9 T_g, 5.0×10^{-5} s^{-1}	7.78	1.579	0.05	0.101	0.2040	2.026
0.9 T_g, 1×10^{-4} s^{-1}	7.78	1.85	0.05	0.109	0.2390	2.18
0.9 T_g, 2×10^{-4} s^{-1}	7.78	2.167	0.05	0.118	0.2800	2.358
0.9 T_g, 3×10^{-4} s^{-1}	7.78	2.41	0.05	0.124	0.3114	2.476
0.9 T_g, 5×10^{-4} s^{-1}	7.78	2.655	0.05	0.1321	0.343	2.642
0.9 T_g, 10^{-3} s^{-1}	7.78	3.089	0.05	0.145	0.399	2.902
0.86 T_g, 10^{-4} s^{-1}	8.32	3.01	0.05	0.147	2.937	0.366
0.89 T_g, 10^{-4} s^{-1}	7.84	2.09	0.05	0.116	2.325	0.266
0.92 T_g, 10^{-4} s^{-1}	7.52	1.456	0.05	0.0972	1.943	0.193
0.95 T_g, 10^{-4} s^{-1}	7.19	1.056	0.05	0.0842	1.684	0.147
0.99 T_g, 10^{-4} s^{-1}	6.80	0.581	0.05	0.0722	1.444	0.085
0.9 T_g, 10^{-4} s^{-1}	7.78	3.08	0.035	0.1089	0.396	3.111
0.9 T_g, 10^{-4} s^{-1}	7.78	2.71	0.040	0.1089	0.3488	2.723
0.9 T_g, 10^{-4} s^{-1}	7.78	2.36	0.045	0.1089	0.3037	2.42
0.9 T_g, 10^{-4} s^{-1}	7.78	1.579	0.05	0.1089	0.2032	2.178
0.9 T_g, 10^{-4} s^{-1}	7.78	1.30	0.06	0.1089	0.1673	1.815
0.9 T_g, 10^{-4} s^{-1}	7.78	0.53	0.08	0.1089	0.0682	1.361
0.9 T_g, 10^{-4} s^{-1}	7.78	0.156	0.10	0.1089	0.0201	1.089
0.9 T_g, 10^{-4} s^{-1}	7.78	Aging	0.11	0.1089	Aging	− 0.0011

permanently stored in the configurational space. As a competent indicator to quantitatively probe the rejuvenation degree, the EED opens a window into exploiting new rejuvenation strategies for glasses.

Acknowledgements This work was supported by the General Project (No. 11972345), the National Outstanding Youth Science Fund Project (No. 12125206), the Major Project (No. 11790292) of National Natural Science Foundation of China (NSFC) and the NSFC Basic Science Center for "Multiscale Problems in Nonlinear Mechanics" (No. 11988102).

Declarations

Conflict of interest The authors declare that they have no conflicts of interest in this work. And we declare that we do not have any commercial

or associative interest that represents a conflict of interest in connection with the work submitted.

References

1. Debenedetti PG, Stillinger FH. Supercooled liquids and the glass transition. Nature. 2001;410(6825):259–67.
2. Goldstein M. Viscous liquids and the glass transition: A potential energy barrier picture. J Chem Phys. 1969;51:3728–39.
3. Charbonneau P, Kurchan J, Parisi G, Urbani P, Zamponi F. Fractal free energy landscapes in structural glasses. Nat Commun. 2014;5(1):3725.
4. Ke HB, Wen P, Peng HL, Wang WH, Greer AL. Homogeneous deformation of metallic glass at room temperature reveals large dilatation. Scripta Mater. 2011;64(10):966–9.
5. Tong Y, Dmowski W, Yokoyama Y, Wang G, Liaw PK, Egami T. Recovering compressive plasticity of bulk metallic glasses by high-temperature creep. Scripta Mater. 2013;69(8):570–3.
6. Haruyama O, Kisara K, Yamashita A, Kogure K, Yokoyama Y, Sugiyama K. Characterization of free volume in cold-rolled Zr55Cu30Ni5Al10 bulk metallic glasses. Acta Mater. 2013;61(9):3224–32.
7. Li S, Zhang JC, Sha ZD. Mechanical behavior of metallic glasses with pressure-promoted thermal rejuvenation. J Alloys Compd. 2020;848:156597.
8. Tong Y, Iwashita T, Dmowski W, Bei H, Egami T. Structural rejuvenation in bulk metallic glasses. Acta Mater. 2015;86(36):240–6.
9. Sun Y, Concustell A, Greer AL. Thermomechanical processing of metallic glasses: extending the range of the glassy state. Nat Rev Mater. 2016;1(9):16039.
10. Ketov SV, Sun YH, Nachum S, Lu Z, Checchi A, Beraldin AR, Bai HY, Wang WH, Louzguine-Luzgin DV, Carpenter MA, Greer AL. Rejuvenation of metallic glasses by non-affine thermal strain. Nature. 2015;524(7564):200–3.
11. Pan J, Wang YX, Guo Q, Zhang D, Greer AL, Li Y. Extreme rejuvenation and softening in a bulk metallic glass. Nat Commun. 2018;9(1):560.
12. Ross P, Küchemann S, Derlet PM, Yu H, Arnold W, Liaw P, Samwer K, Maaß R. Linking macroscopic rejuvenation to nano-elastic fluctuations in a metallic glass. Acta Mater. 2017;138:111–8.
13. Tong Y, Dmowski W, Bei H, Yokoyama Y, Egami T. Mechanical rejuvenation in bulk metallic glass induced by thermo-mechanical creep. Acta Mater. 2018;148:384–90.
14. Ding G, Li C, Zaccone A, Wang WH, Lei HC, Jiang F, Ling Z, Jiang MQ. Ultrafast extreme rejuvenation of metallic glasses by shock compression. Sci Adv. 2019;5(8):eaaw6249.
15. Hufnagel TC. Metallic glasses: Cryogenic rejuvenation. Nat Mater. 2015;14(9):867–8.
16. Harmon JS, Demetriou MD, Johnson WL, Samwer K. Anelastic to plastic transition in metallic glass-forming liquids. Phys Rev Lett. 2007;99(13):135502.
17. Phan AD, Zaccone A, Lam VD, Wakabayashi K. Theory of pressure-induced rejuvenation and strain hardening in metallic glasses. Phys Rev Lett. 2021;126(2):025502.
18. Kamrin K, Bouchbinder E. Two-temperature continuum thermomechanics of deforming amorphous solids. J Mech Phys Solids. 2014;73:269–88.
19. Rittel D, Wang ZG, Merzer M. Adiabatic shear failure and dynamic stored energy of cold work. Phys Rev Lett. 2006;96(7):075502.
20. Viasnoff V, Lequeux F. Rejuvenation and overaging in a colloidal glass under shear. Phys Rev Lett. 2002;89(6):065701.
21. Zhang M, Wang YM, Li FX, Jiang SQ, Li MZ, Liu L. Mechanical Relaxation-to-Rejuvenation Transition in a Zr-based Bulk Metallic Glass. Sci Rep. 2017;7(1):625.
22. Jiang MQ, Wilde G, Dai LH. Origin of stress overshoot in amorphous solids. Mech Mater. 2015;81:72–83.
23. Park K-W, Lee C-M, Wakeda M, Shibutani Y, Falk ML, Lee J-C. Elastostatically induced structural disordering in amorphous alloys. Acta Mater. 2008;56(19):5440–50.
24. Dmowski W, Yokoyama Y, Chuang A, Ren Y, Umemoto M, Tsuchiya K, Inoue A, Egami T. Structural rejuvenation in a bulk metallic glass induced by severe plastic deformation. Acta Mater. 2010;58(2):429–38.
25. Argon AS. Plastic deformation in metallic glasses. Acta Metall. 1979;27(1):47–58.
26. Lu YZ, Jiang MQ, Lu X, Qin ZX, Huang YJ, Shen J. Dilatancy of shear transformations in a colloidal glass. Phys Rev Appl. 2018;9(1):014023.
27. Argon AS, Demkowicz MJ. What Can plasticity of amorphous silicon tell us about plasticity of metallic glasses? Metall Mater Trans A. 2008;39(8):1762–78.
28. Lemaître A. Rearrangements and dilatancy for sheared dense materials. Phys Rev Lett. 2002;89(19):195503.
29. Spaepen F. A microscopic mechanism for steady state inhomogeneous flow in metallic glasses. Acta Metall. 1977;25(4):407–15.
30. Heggen M, Spaepen F, Feuerbacher M. Creation and annihilation of free volume during homogeneous flow of a metallic glass. J Appl Phys. 2005;97(3):033506.
31. Ding J, Li L, Wang N, Tian L, Asta M, Ritchie RO, Egami T. Universal nature of the saddle states of structural excitations in metallic glasses. Mater Today Phys. 2021;17:100359.
32. Jiang MQ, Wilde G, Dai LH. Shear band dilatation in amorphous alloys. Scripta Mater. 2017;127:54–7.
33. Sun X, Ding G, Mo G, Dai LH, Jiang MQ. Dilatancy signatures of amorphous plasticity probed by X-ray synchrotron radiation. Intermetallics. 2019;107:34–8.
34. Miyazaki N, Wakeda M, Wang Y-J, Ogata S. Prediction of pressure-promoted thermal rejuvenation in metallic glasses. npj Comput Mater. 2016;2(1):16013.
35. Langer JS, Manning ML. Steady-state, effective-temperature dynamics in a glassy material. Phys Rev E. 2007;76(5):056107.
36. Yang Z-Y, Dai L-H. Giant configurational softening controls atomic-level process of shear banding in metallic glasses. Phys Rev Mater. 2021;5(12):123602.
37. Yang Z-Y, Wang Y-J, Dai L-H. Susceptibility of shear banding to chemical short-range order in metallic glasses. Scripta Mater. 2019;162:141–5.
38. Lacks DJ, Osborne MJ. Energy landscape picture of overaging and rejuvenation in a sheared glass. Phys Rev Lett. 2004;93(25):255501.
39. Tang XC, Nguyen T, Yao XH, Wilkerson JW. A cavitation and dynamic void growth model for a general class of strain-softening amorphous materials. J Mech Phys Solids. 2020;141:104023.
40. Cao P, Short MP, Yip S. Understanding the mechanisms of amorphous creep through molecular simulation. Proc Natl Acad Sci U S A. 2017;114(52):13631–6.
41. Zhu W, Liu J, Mao S, Wei X. A new continuum model for viscoplasticity in metallic glasses based on thermodynamics and its application to creep tests. J Mech Phys Solids. 2021;146:104216.
42. Schinasi-Lemberg E, Regev I. Annealing and rejuvenation in a two-dimensional model amorphous solid under oscillatory shear. Phys Rev E. 2020;101(1):012603.
43. Pan J, Ivanov YP, Zhou WH, Li Y, Greer AL. Strain-hardening and suppression of shear-banding in rejuvenated bulk metallic glass. Nature. 2020;578(7796):559–62.
44. de Hey P, Sietsma J, van den Beukel A. Structural disordering in amorphous Pd40Ni40P20 induced by high temperature deformation. Acta Mater. 1998;46(16):5873–82.
45. Jiang MQ, Wang WH, Dai LH. Prediction of shear-band thickness in metallic glasses. Scripta Mater. 2009;60(11):1004–7.

46. Greer AL, Cheng YQ, Ma E. Shear bands in metallic glasses. Mater Sci Eng R. 2013;74(4):71–132.
47. Jiang MQ, Dai LH. On the origin of shear banding instability in metallic glasses. J Mech Phys Solids. 2009;57(8):1267–92.
48. Jiang MQ, Dai LH. Shear-band toughness of bulk metallic glasses. Acta Mater. 2011;59(11):4525–37.
49. Wang C, Yang ZZ, Ma T, Sun YT, Yin YY, Gong Y, Gu L, Wen P, Zhu PW, Long YW, Yu XH, Jin CQ, Wang WH, Bai HY. High stored energy of metallic glasses induced by high pressure. Appl Phys Lett. 2017;110(11):111901.